Separation Science and Technology
Publication details, including instructions for authors and subscription information:
http://www.informaworld.com/smpp/title~content=t713708471

Models and Experiments on Electrokinetic Removal of Pb(II) from Kaolinite Clay

Soon-Oh Kim[ab]; Jae-Jin Kim[b]; Kyoung-Woong Kim[c]; Seong-Taek Yun[a]
[a] Department of Earth and Environmental Sciences, Korea University, Seoul, Republic of Korea [b] Climate Environment System Research Center, Seoul National University, Seoul, Republic of Korea [c] Department of Environmental Science and Engineering, Gwangju Institute of Science and Technology (GJIST), Gwangju, Republic of Korea

Online publication date: 08 July 2010

To cite this Article Kim, Soon-Oh , Kim, Jae-Jin , Kim, Kyoung-Woong and Yun, Seong-Taek(2005) 'Models and Experiments on Electrokinetic Removal of Pb(II) from Kaolinite Clay', Separation Science and Technology, 39: 8, 1927 — 1951
To link to this Article: DOI: 10.1081/SS-120030775
URL: http://dx.doi.org/10.1081/SS-120030775

SEPARATION SCIENCE AND TECHNOLOGY
Vol. 39, No. 8, pp. 1927–1951, 2004

Models and Experiments on Electrokinetic Removal of Pb(II) from Kaolinite Clay

Soon-Oh Kim,[1,#] Jae-Jin Kim,[2] Kyoung-Woong Kim,[3] and Seong-Taek Yun[1,*]

[1]Department of Earth and Environmental Sciences, Korea University, Seoul, Republic of Korea
[2]Climate Environment System Research Center, Seoul National University, Seoul, Republic of Korea
[3]Department of Environmental Science and Engineering, Gwangju Institute of Science and Technology (GJIST), Gwangju, Republic of Korea

ABSTRACT

Numerical and experimental studies were conducted to understand the Pb(II) transport through the fine-grained soil of low-hydraulic permeability under electrical fields. The numerical model involved multi-

[#]Current address: Climate Environment System Research Center, Seoul National University, Seoul, Republic of Korea.
*Correspondence: Seong-Taek Yun, Department of Earth and Environmental Sciences, Korea University, Seoul 136-701, Republic of Korea; Fax: +82-2-3290-3189; E-mail: styun@korea.ac.kr.

DOI: 10.1081/SS-120030775 0149-6395 (Print); 1520-5754 (Online)

component species transport under coupled chemical and electrical potential gradients and incorporated several chemical reactions occurring within the kaolinite clay during the processing, such as aqueous phase reaction, adsorption, and precipitation. The model also emphasized physicochemical factors such as soil pH and zeta potential, which vary with location and processing time and directly affect the transport of species. The model predicted the soil pH distribution as well as the transport and fate of Pb(II). The validity of the model was confirmed by comparing the model prediction with experimental results. The model simulation and experimental results, using unenhanced and enhanced tests, clearly demonstrated that the change in pH within the soil specimen is a crucial factor affecting the solubilities of Pb(II) and its adsorption to the soil, resulting in governing the removal of Pb(II) by electrical fields. This study confirms that enhancement methods should be considered to control soil pH, in order to improve electrokinetic removal of heavy metal contaminants.

Key Words: Kaolinte clay; Lead [Pb(II)]; Electrokinetic removal; Soil pH; Enhancement.

INTRODUCTION

Recently, it has been reported that soil contamination by heavy metals, which cause serious human health problems, is increasing in various sites including residential areas near industrial complexes and reservoirs of drinking water. However, technologies for decontaminating these sites have not been well developed, particularly for fine-grained soils of low hydraulic permeability such as clay. Among newly developed techniques, electrokinetic processing has proved to be one of the most promising techniques in removing contaminants from low-permeability soils.[1–11] Electrokinetic remediation involves passage of direct current in the order of mA/cm^2 through soil to remove/extract radionuclides, heavy metals, certain organic compounds, or mixed inorganic and organic wastes from soils and slurries. The major advantages of the electrokinetic remediation include:[12] (a) a specific applicability to low permeability soils, e.g., clayey soils. Such soils have a greater ability to adsorb pollutants, and therefore are resistant to common in-situ remedial techniques, such as the pump-and-treat method, which would require a very high-hydraulic gradient to be efficient; (b) a high degree of controllability of flow direction, unlike soil flushing; (c) the capability of removing a wide range of contaminants, e.g., heavy metals, radionuclides, and organic compounds; and (d) a low electric power consumption. Until now, numerous researches using numerical modeling, laboratory and pilot-scale experiments,

Marcel Dekker, Inc.
270 Madison Avenue, New York, New York 10016

and field applications have evaluated and assessed electrokinetic processing. Drawbacks and imperfections of those studies are well documented by Page and Page[10] and Kim.[13]

Lead has been considered as one of the most hazardous contaminants together with cadmium, copper, mercury, nickel, and zinc. The divalent form (+2 oxidation state) is the most common and is capable of replacing calcium, strontium, barium, and potassium in soils. Lead is present in uncontaminated soils at the range of 10–84 mg/kg (worldwide means),[14] but much higher concentrations have been reported in many areas as a consequence of anthropogenic emissions such as mining and smelting activities, manures, paints, batteries, and vehicle exhausts.[15] Once lead is released into the environment, it has a long residence time compared with most other pollutants, because lead and its compounds tend to easily accumulate in soils and sediments due to their low solubility and relative freedom from microbial degradation.[15] In addition, lead is the least mobile heavy metal in soils, especially under reducing or nonacid conditions. A number of researchers have demonstrated that lead has strong affinity with and high selectivity onto reactive sorbents such as goethite and other hydrous oxides as a result of adsorption, ion exchange, and complexation.[16–18] Furthermore, lead is toxic to human health, and it is well known that lead poisoning gives rise to mental impairment in young children, anemia, various digestive disorders, and central nervous system effects. In addition, concentrations of lead in many environments are sufficiently high as to pose a potential risk to human health. Lead was selected as a target heavy metal in this study due to its distinct geochemical characteristics and toxicity.

In this study, we developed one-dimensional numerical modeling for coupled multicomponent species transport through kaolinite clay under chemical and electrical gradients. The model included chemical reactions such as electrolysis of water, aqueous phase reaction, adsorption, and precipitation. However, the purpose of the model was not to evaluate general features of an electrokinetic system, but to investigate the specific system of the electrokinetic transport of lead in kaolinite at laboratory scale. The model predictions were validated by comparison with experimental results. Based on the numerical simulations and experimental results, the most important factor controlling the species transport was evaluated.

THEORETICAL

If electrical and chemical gradients are imposed on a soil–water-contaminant system, fluxes of fluid and mass are initiated through soil media. The fluid flux due to electrical gradient, termed electroosmosis, can

MARCEL DEKKER, INC.
270 Madison Avenue, New York, New York 10016

be expressed using the Helmholtz–Smoluchowski theory:[14,19,20]

$$J_w = -k_{eo}\nabla\Phi \tag{1a}$$

The value of k_{eo} is a function of zeta potential, viscosity of fluid, porosity, and electrical permeability of soil, and is given by:[14,21]

$$k_{eo} = \frac{\varepsilon\zeta n}{\mu} \tag{1b}$$

According to the Helmholtz–Smoluchowski theory, electroosmotic permeability coefficient (k_{eo}) is independent of pore size, unlike the hydraulic conductivity (k_h). Published figures for k_{eo}, determined experimentally, show that it is relatively independent of soil type and values generally fall in the narrow range between 10^{-9} and $10^{-8}\,m^2/V$ sec compared with the k_h values between 10^{-13} and $10^{-5}\,m/sec$.[10,14] Therefore, an electrical gradient is more effective than a hydraulic gradient in moving liquid through fine-grained soils, and it is assumed that the hydraulically driven advection flow is negligible, i.e., no hydraulic head exists, in this study. The detailed discussion of the k_{eo} value is presented in the later section, Model Predictions.

Mass flux of chemical species is caused by different mechanisms, and the total mass flux can be estimated by considering the mass transport by diffusion, electromigration, and electroosmotic advection in the system under chemical and electrical gradients:[14,19,22,23]

$$J_i = D_i^*\nabla(-c_i) + c_i(u_i^* + k_{eo})\nabla(-\Phi) \tag{2}$$

The effective diffusion coefficient in the porous medium, D_i^*, is expressed by the respective diffusion coefficient in free solution, D_i:[20,23,24]

$$D_i^* = n\tau D_i \tag{3}$$

Typical values of τ are reported in the range 0.01–0.67.[25–27] Hence, the mass transport due to diffusion in porous media is slower than the mass transport due to diffusion in free or aqueous solution. The effective ionic mobility, u_i^*, describes the velocity of the ion in soil pores under electric field. Even though the accurate measurement of the value is significantly difficult, the value can be estimated theoretically using the Nernst–Einstein relation between the molecular diffusion coefficient, D_i, and the ionic mobility, u_i:[19,23,28]

$$u_i^* = \frac{D_i^* z_i F}{RT} = n\tau u_i \tag{4}$$

The values of ionic mobilities and effective ionic mobilities are negative for anions but positive for cations.

MARCEL DEKKER, INC.
270 Madison Avenue, New York, New York 10016

A time-dependent equation for the conservation of mass is used to describe transient mass transport of species i:

$$n\frac{\partial c_i}{\partial t} = -\nabla J_i + nR_i \tag{5}$$

The production in Eq. (5), R_i, can be simplified using algebraic equations describing chemical reactions such as aqueous phase, adsorption, and precipitation reactions:

$$R_i = R_i^{\text{aq}} + R_i^{\text{ad}} + R_i^{\text{p}} \tag{6}$$

All the chemical reactions involved are assumed to be under instantaneous equilibrium state. The water-autoionization reaction is taken into account as the aqueous phase reaction. In addition, the linear adsorption isotherm of Pb(II) onto kaolinite clay was determined by adsorption experiments, and was used to describe adsorption reaction. This empirically determined adsorption isotherm of Pb(II) onto kaolinite clay is fully explained in the later section, "Model Predictions". Finally, the solubility product of lead hydroxide, $K_{\text{sp}}^{\text{Pb(OH)}_2}$, is introduced to model precipitation reaction. Herein, the algebraic equations describing the aqueous phase reaction and precipitation are as follows:

$$c_{\text{H}}c_{\text{OH}} = K_{\text{w}} = 10^{-14} \tag{7a}$$

$$c_{\text{OH}}^2 c_{\text{Pb}} \le K_{\text{sp}}^{\text{Pb(OH)}_2} = 1.2 \times 10^{-15} \tag{7b}$$

The total change of OH^- concentration due to both reactions is obtained by combining the water-autoionization reaction and precipitation reaction:

$$\Delta c_{\text{OH}} = \Delta c_{\text{H}} + 2\Delta c_{\text{Pb}} \tag{8a}$$

$$R_{\text{OH}} = R_{\text{H}}^{\text{aq}} + 2R_{\text{Pb}}^{\text{p}} \tag{8b}$$

For one-dimensional implementation, four initial conditions and eight boundary conditions are required for four partial differential equations (PDEs) describing the transport of four chemical species in the soil pore fluid, i.e., Pb^{2+}, H^+, OH^-, and NO_3^-. Additionally, four algebraic equations are used to describe the chemical reactions of Pb^{2+} in the pore fluid such as Eqs. (7a), (7b), and (8b), and the adsorption isotherm of Pb^{2+}. Imposing the electroneutrality constraint on the system, one PDE disappears, thus the total number of PDEs decreased to three. Therefore, three initial conditions and six boundary conditions are required. Boundary conditions for PDEs describing species transport are given by species flux, and electrolysis reactions occurring in the electrodes.

Marcel Dekker, Inc.
270 Madison Avenue, New York, New York 10016

Transport of Pb(II) under electrical and chemical gradients is described as:

$$n\frac{\partial c_{Pb}}{\partial t} = D^*_{Pb}\frac{\partial^2 c_{Pb}}{\partial x^2} + (u^*_{Pb} + k_{eo})\frac{\partial c_{Pb}}{\partial x}\frac{\partial \Phi}{\partial x} + c_{Pb}(u^*_{Pb} + k_{eo})\frac{\partial^2 \Phi}{\partial x^2} - R^{ad}_{Pb} - R^{P}_{Pb} \quad (9)$$

Boundary conditions for Eq. (10) are expressed as:

$$J_{Pb}|_{x=0} = 0 \quad - D^*_{Pb}\frac{\partial c_{Pb}}{\partial x} - c_{Pb}(u^*_{Pb} + k_{eo})\left.\frac{\partial \Phi}{\partial x}\right|_{x=0} = 0 \quad (10a)$$

$$J_{Pb}|_{x=L} = c_{Pb}J_w \quad - D^*_{Pb}\frac{\partial c_{Pb}}{\partial x} - c_{Pb}(u^*_{Pb} + k_{eo})\left.\frac{\partial \Phi}{\partial x}\right|_{x=L} = -c_{Pb}k_{eo}\frac{\partial \Phi}{\partial x} \quad (10b)$$

The boundary conditions for H^+ and OH^- can be expressed using the amount of each ion produced by electrolysis reactions at the electrodes and transient volumes of both electrode reservoirs changed in time due to electroosmotic flow. In addition, the Faraday efficiency determined empirically is used for the generation of hydrogen and hydroxide ions. The volume changes in both electrode reservoirs are related to electroosmotic flow estimated using electroosmotic permeability coefficient (k_{eo}), as shown in Eq. (1a), whose k_{eo} value can be calculated by the empirically determined relation between zeta potential (ζ) and pH. Therefore, the boundary concentrations of hydrogen and hydroxyl ions can be expressed as a function of reservoir volume and processing time. The electric potential gradient in the numerical simulation is assumed to be constant across the soil bed throughout the simulation. As a matter of fact, the local voltage gradient is determined by the local conductivity, and this is a major feature of electrokinetic system. In order to complete the simulation, however, a complicated and tremendous task should be required, because the local conductivity should be expressed as a function of the local concentrations of ions involved, which are unknown values in the model. There has been numerous research about the procedure to numerically solve this problem so far.[20,29–31] To avoid the complexity, however, the value of constant electrical gradient used in this model simulation was empirically determined after several experiments. The average value of voltage gradients measured in the experimental studies is used in the numerical simulation.

MARCEL DEKKER, INC.
270 Madison Avenue, New York, New York 10016

The PDE expressing H^+ transport is given by:

$$R_H^d \frac{\partial c_H}{\partial t} = D_H^* \frac{\partial^2 c_H}{\partial x^2} + (u_H^* + k_{eo}) \frac{\partial c_H}{\partial x} \frac{\partial \Phi}{\partial x} + c_H (u_H^* + k_{eo}) \frac{\partial^2 \Phi}{\partial x^2} - R_H^{aq} \quad (11)$$

There is no specific study available on sorption of H^+on kaolinite. Alshawabkeh and Acar[20] suggested that a value of R_H^d was 4.6, based on the results of pilot-scale tests using kaolinite conducted by Acar and Alshawabkeh.[32] The retardation factor of H^+, R_H^d, was determined in this study by several experiments, which followed the method suggested by Alshawabkeh and Acar.[20] The average value of 4.0 was selected as R_H^d in this numerical modeling. Boundary conditions for Eq. (11) are expressed as:

$$c_H|_{x=0} = c_H^{anode} + \frac{(I \eta t A)}{F(V_{anode} - V_{eo})} \quad (12a)$$

$$c_H|_{x=L} = \frac{10^{-14}}{c_{OH}} \quad (12b)$$

The value of η represents the lumped parameter used to account for the buffering in the reservoirs, efficiency of electrolysis, etc. It was experimentally measured in this study, and ranged from 0.18 to 0.20. In the numerical modeling, the average value of 0.19 was used.

The OH^+ transport equation is given by:

$$n \frac{\partial c_{OH}}{\partial t} = D_{OH}^* \frac{\partial^2 c_{OH}}{\partial x^2} + (u_{OH}^* + k_{eo}) \frac{\partial c_{OH}}{\partial x} \frac{\partial \Phi}{\partial x} + c_{OH} (u_{OH}^* + k_{eo}) \frac{\partial^2 \Phi}{\partial x^2} - R_{OH}^{aq} \quad (13)$$

Boundary conditions are:

$$c_{OH}|_{x=0} = \frac{10^{-14}}{c_H} \quad (14a)$$

$$c_{OH}|_{x=L} = c_{OH}^{cathode} + \frac{(I \eta t A)}{F(V_{cathode} - V_{eo})} \quad (14b)$$

Finally, it is unnecessary to describe the transport equation of NO_3^-, because the time-dependent concentrations of NO_3^- in local points can be obtained by imposing the electrical neutrality constraint in the system:

$$c_{NO} = -\frac{\sum_{k=1}^{3} z_k c_k}{z_{NO}} \quad (15)$$

where $k = 1$, 2, and 3 correspond to Pb^{2+}, H^+, and OH^-, respectively.

MARCEL DEKKER, INC.
270 Madison Avenue, New York, New York 10016

Finite difference method (FDM) and explicit forward time and centered space (FTCS) schemes were used to solve the developed governing equations describing the transport of fluid and contaminant through kaolinite clay under electrical fields numerically. Two numerical programs were developed to simulate the transport of Pb(II) in both unenhanced and enhanced electrokinetic processing. In the modeling for enhanced electrokinetic processing, the conditionings of anolyte and catholyte were designed to boost hydrogen ions in anolyte and to buffer hydroxyl ions in catholyte with 0.001 M (pH = 3) and 0.1 M (pH = 1) nitric acid solutions, respectively.

EXPERIMENTAL

The experimental apparatus consists of four principal parts: soil cell, electrode compartments, electrolyte solution reservoirs, and power supply (Fig. 1). The acryl soil cell measures 10 cm × 10 cm × 15 cm with a volume of 1500 cm^3. The soil was separated from the electrode compartment by two sheets of porous polyethylene-terephthalate (PET) filter, preventing soil particles from flowing into the electrode compartments. The anode was made from platinum plate (10 cm × 10 cm) to prevent the introduction of extraneous products due to electrolytic reaction of the electrode surface,

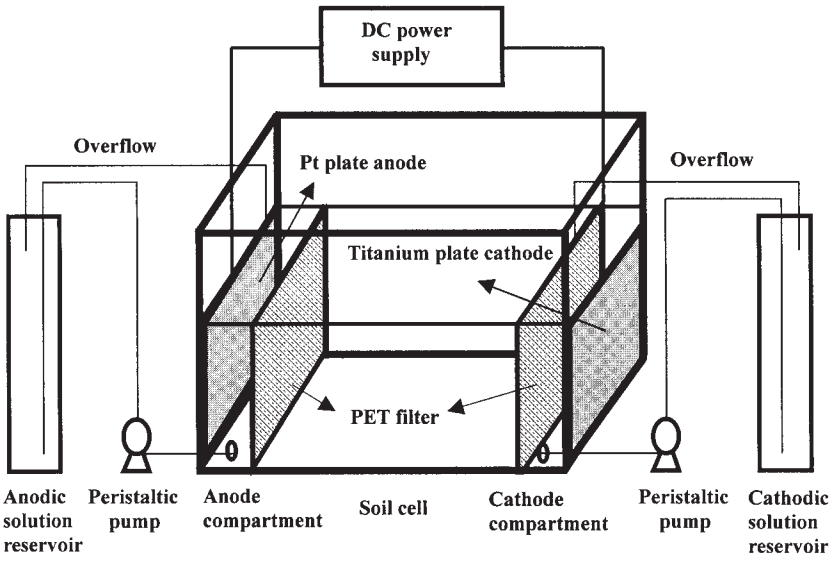

Figure 1. Schematic diagram of experimental apparatus.

whereas titanium plate (10 cm × 10 cm) was used as the cathode. The electrode compartments containing 500 mL of electrolyte solution were connected to tubes for supplying the purge solutions and for withdrawing the contaminant solution, ensuring that sufficient volume was present to avoid sudden variation of each electrolyte solution. In addition, the compartments also contained vents for discharging the oxygen and hydrogen that are produced by the electrolysis of water at both electrodes. Two mass cylinders (2 L volume) were used as electrolyte solution reservoirs to measure the volume of water transported. The electrolyte solutions were recirculated in both electrode compartments by peristaltic pumps (Masterflex, 1–100 rpm, 3 heads), and a BIORAD DC power supply (model PowerPac 200, 5–200 V, 0.01–2 A, 200 W) was used.

Kaolinite clay was used in this experimental study, since it is one of the most common clay soils in Korea and frequently used as soil media in the researches on electrokinetic processing due to its low hydraulic permeability and low activity on heavy metals among various clayey soils. The soil specimen was prepared by spiking kaolinite with 3 L of 14,000 mg/L Pb(II) solution, which was prepared by dissolving 67.82 g $Pb(NO_3)_2$ in 3 L of distilled water. The resultant kaolinite specimen contained 7000 mg/kg of dry soil (6.77 meq/100 g of dry soil) of Pb(II). In order to examine whether electrokinetic remediation technology would remove the contaminants adsorbed by the clay mineral, it was designed to load the Pb(II) at the level of 7000 mg/kg, which was below the maximum adsorbed concentration (10,204 mg/kg of dry soil, 9.85 meq/100 g of dry soil) in kaolinite. Therefore, all the Pb(II) species initially existed in adsorbed forms in the prepared kaolinite soil. The slurries of kaolinite prepared were mixed mechanically for 1 hr with an electric stirrer, and these mixtures were allowed to settle down for more than 1 week in order to attain a uniform distribution of contaminant and to complete adsorption in the soil samples. Five grams of six samples were then taken from the prepared soils for the determination of initial concentration of Pb(II).

The soil cell was horizontally placed to diminish hydraulic gradients. After treatment, five samples were obtained from the soil bed using a stainless steel sampler (diameter: 1.2 cm) at every 3 cm to analyze the residual Pb(II) concentrations and final soil pH. The samples taken were extracted by Korea Standard Testing Method (KSTM); wet soil samples were dried at 105°C, 50 mL of 0.1 N HCl solution was added into 5 g of each dry soil sample (dilution factor: 10) and then agitated (100 rpm, 30°C, and 1 hr). The solutions were then analyzed by ICP-AES (ICP-AES, Thermo Jarrel Ash, USA).

Two different types of tests, unenhanced (conventional) and enhanced tests, were undertaken to compare the effectiveness of the two processes. Table 1 summarizes the parameters used in each experiment. Distilled water was used as

Table 1. Experimental design of the unenhanced and enhanced tests.

	Unenhanced test	Enhanced test
Soil specimen	Kaolinite clay	
Contaminant	Pb(II)	
Initial concentration	7000 mg/kg (6.77 meq/100 g of dry soil)	
Length (cm) and cross-sectional area (cm^2) of soil cell	15 and 100	
Applied current (mA)	100	
Applied current density (mA/cm^2)	1	
Duration (hr)	96	72
Anode purging solution	Distilled water	0.001 M HNO_3
Cathode electrolyte solution	Distilled water	0.1 M HNO_3

anodic and cathodic electrolyte solutions in the unenhanced test, whereas 0.001 and 0.1 M HNO_3 were used in the enhanced test. One of the main drawbacks of the conventional (unenhanced) electrokinetics is precipitation of hydroxides near the cathode due to generation of hydroxyl ions by the electrolysis of water occurring at the cathode and migration into soil specimen, resulting in decrease of the effectiveness of the technology. In order to prevent this precipitation, 0.1 M HNO_3 was used as catholyte for buffering those hydroxyl ions and maintaining the pH below 3. In addition, 0.001 M HNO_3 anolyte was used in the enhanced tests to boost the level of hydrogen ions and enhance the reactivity of hydrogen ions with Pb(II) species, for the purpose of both decreasing the treatment time and increasing the removal efficiency.

RESULTS AND DISCUSSION

Model Predictions

Parameters and constants related to the kaolinite soil were evaluated, either through laboratory tests or through approximation using literature data (Table 2). Porosity and bulk density of kaolinite soil were experimentally determined. The tortuosity factor (τ) for kaolinite modeled was not determined experimentally, but a value of 0.40 was used in this study. In general, typical values of τ vary in the range 0.01–0.67 according to the soil type, and vary over a narrow range between 0.12 and 0.50 for kaolinite.[24,26,27] The electroosmotic permeability coefficient in Eq. (1), k_{eo}, is a soil property indicating the hydraulic flow velocity under a unit electrical gradient. Measurement of k_{eo} can be made by determination of the flow rate of water through a soil sample

MARCEL DEKKER, INC.
270 Madison Avenue, New York, New York 10016

Table 2. Measured parameters and related constants used in numerical modeling.

Parameters or constants	Program	
	PB-EKP	PB-ENEKP
Operational condition	Unenhanced	Enhanced
Number of species	4	
Length of soil specimen (m)	0.15	
Number of sections	61	
Stability criteria	0.001	
Time step size (sec)	1	
Porosity (n)	0.48	
Bulk density (ρ, mg/m^3)	1.3	
Tortuosity factor (τ)	0.4	
Initial soil pH	5.4	
Initial zeta potential (ζ, mV)	-8.70	
Initial electroosmotic permeability coefficient (k_{eo}, m^2/V sec)	3.66×10^{-9}	
Electrical permittivity (ε, C/V m)	7.0×10^{-10}	
Viscosity of fluid (μ, C V sec/m^3)	0.001	
Initial concentration of Pb(II) (mol/m^3)	67.568	
Electrical potential gradient (V/m)	40	

of known length and cross-sectional area under a known electrical gradient. From a number of experimental results, it is known that k_{eo} is generally in the range of 1×10^{-9}–1×10^{-8} m^2/V sec and k_{eo} is around 1×10^{-9} m^2/V sec for most clays.[9,14] It is noteworthy that the k_{eo} value is changed during electrokinetic processing, since zeta potential (ζ) of the soil medium varies with the soil pH change due to the acid and/or base front migration from the anode and cathode, respectively. However, the values of k_{eo} and ζ have been treated as constants in numerous model studies.[21–23,32–35] Meanwhile, Eykholt and Daniel[21] and Eykholt[34] suggested the relationship between the change of pH and zeta potential. The empirical relation was suggested as:[21,34]

$$\zeta(mV) = -38.6 + 281e^{-0.48\ \mathrm{pH}} \tag{16}$$

They did not directly measure the zeta potential, and used a regression method using the data from Lorenz.[35] In this study, the pH-dependent zeta potentials were experimentally determined using the instrument operated by electrophoretic light scattering (ELS-8000, Otsuka Electronics, Japan). Then, the relation between pH and ζ was empirically evaluated, and finally the pH-dependent values of ζ were calculated at local points across the soil

specimen during the modeling. Accordingly, the k_{eo} value was determined from the calculated value of ζ based on Eq. (1b). The empirical relation between pH and ζ is presented in Fig. 2, compared with the relation suggested by Eykholt and Daniel.[21] This relation was used in the modeling to predict the electroosmotic flow at each local point. The effective diffusion coefficients and effective ionic mobilities of species are presented in Table 3, which were calculated by the diffusion coefficients and ionic mobilities at infinite dilution. The algebraic equation describing the adsorption of Pb(II) onto kaolinite was developed based on the linear and pH-dependent adsorption isotherm determined empirically. The adsorption edge of Pb(II) and the linear relation between pH and adsorption are presented in Fig. 3(a) and (b), respectively. This relation was used for the calculation of adsorbed concentrations of metal species in the model.

Soil pH values across the electrodes change from as low as 2 to as high as 12 with time in the unenhanced simulation [Fig. 4(a)] whereas pH values of the enhanced simulation show different trends in the region near the cathode [Fig. 4(b)]. The pH jump point after a 1-day run is observed in the region near the middle of the soil bed (normalized distance from anode is about 0.67), and it migrates toward the cathodic side with time, as shown in Fig. 4(a). It is caused by the consumption of hydroxyl ions migrating from the cathodic boundary as a result of the water production with hydrogen ions and the precipitation

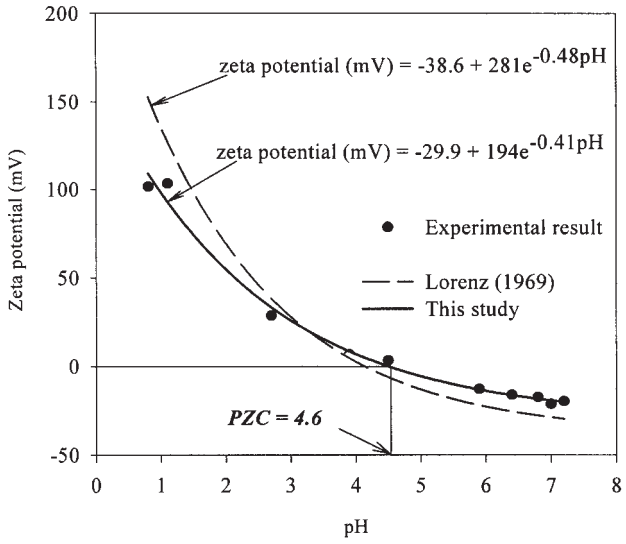

Figure 2. Empirical relation between pH and zeta potential (ζ).

Table 3. Effective diffusion coefficients and effective ionic mobilities used in numerical modeling.

Species	Diffusion coefficient, D_i (m^2/sec)[a]	Ionic mobility, u_i (m^2/V sec)[a]	Effective diffusion coefficient, D_i^* (m^2/sec)	Effective ionic mobility, u_i^* (m^2/V sec)
Pb^{2+}	9.45×10^{-10}	7.36×10^{-8}	1.81×10^{-10}	1.41×10^{-8}
H^+	93.1×10^{-10}	36.25×10^{-8}	17.88×10^{-10}	6.96×10^{-8}
OH^-	52.7×10^{-10}	20.58×10^{-8}	10.12×10^{-10}	3.95×10^{-8}
NO_3^-	19.0×10^{-10}	7.44×10^{-8}	3.65×10^{-10}	1.43×10^{-8}

Note: $D_i^* = D_i n\tau$ and $u_i^* = u_i n\tau$, where $n = 0.48$ and $\tau = 0.4$.
[a]Data from Mitchell[14] and Alshawabkeh.[23]

reaction with aqueous phase Pb(II) species. The rate of the precipitation reaction in the initial stage is not great due to the small amount of aqueous phase Pb(II) species, since Pb(II) has very strong adsorption affinity onto kaolinite surface even in low pH conditions, i.e., almost 60% of total Pb(II) exists as adsorbed forms in the condition of pH = 3, as presented in Fig. 3(b). In other words, there is no precipitation reaction in the initial stage of simulation, since all the Pb(II) species are partitioned in the adsorbed forms, i.e., the initial concentration of the aqueous phase species is zero. Therefore, the hydroxyl ions migrate from the cathode into the soil bed, and the pH jump point appears near the middle of the soil bed in the early stage of the simulation. However, hydroxyl ions are consumed due to precipitation reaction with the aqueous Pb(II) species, as the adsorbed lead species are desorbed and/or converted into aqueous species and those aqueous species migrate towards the cathode. Accordingly, the pH jump point moves towards the cathodic side, and finally it appears at the region very close to the cathode (at a normalized distance of 0.79). On the contrary, the soil pH near the cathode does not increase in the enhanced simulation, since the hydroxyl ions are buffered by the acidic solution in the cathodic boundary and do not migrate into the soil bed. The final soil pH near the cathode is observed below the initial soil pH 5.4.

The concentration profiles of different forms of Pb(II) for each simulation are shown in Figs. 5 and 6. The initial total concentrations of Pb(II) in both tests are equal (67.568 mol/m^3), and all the Pb(II) species initially exist as adsorbed forms. Accordingly, the initial concentration of the aqueous phase species is zero across the soil bed. This adsorbed species can be transported only if the species are released in the pore fluid with the decrease of soil pH. As the acid front transports from the anode to the cathode, the concentration of the aqueous species increases as a result of the desorption of the

Marcel Dekker, Inc.
270 Madison Avenue, New York, New York 10016

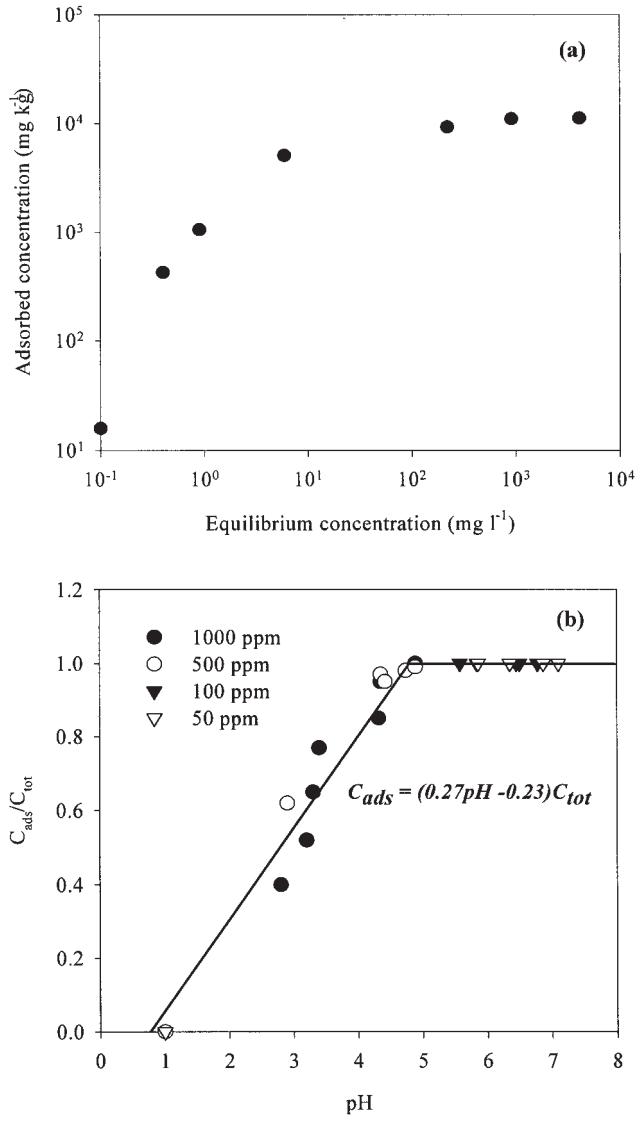

Figure 3. Experimental result of Pb(II) adsorption onto kaolinte: (a) adsorption edge and (b) linear adsorption isotherm.

MARCEL DEKKER, INC.
270 Madison Avenue, New York, New York 10016

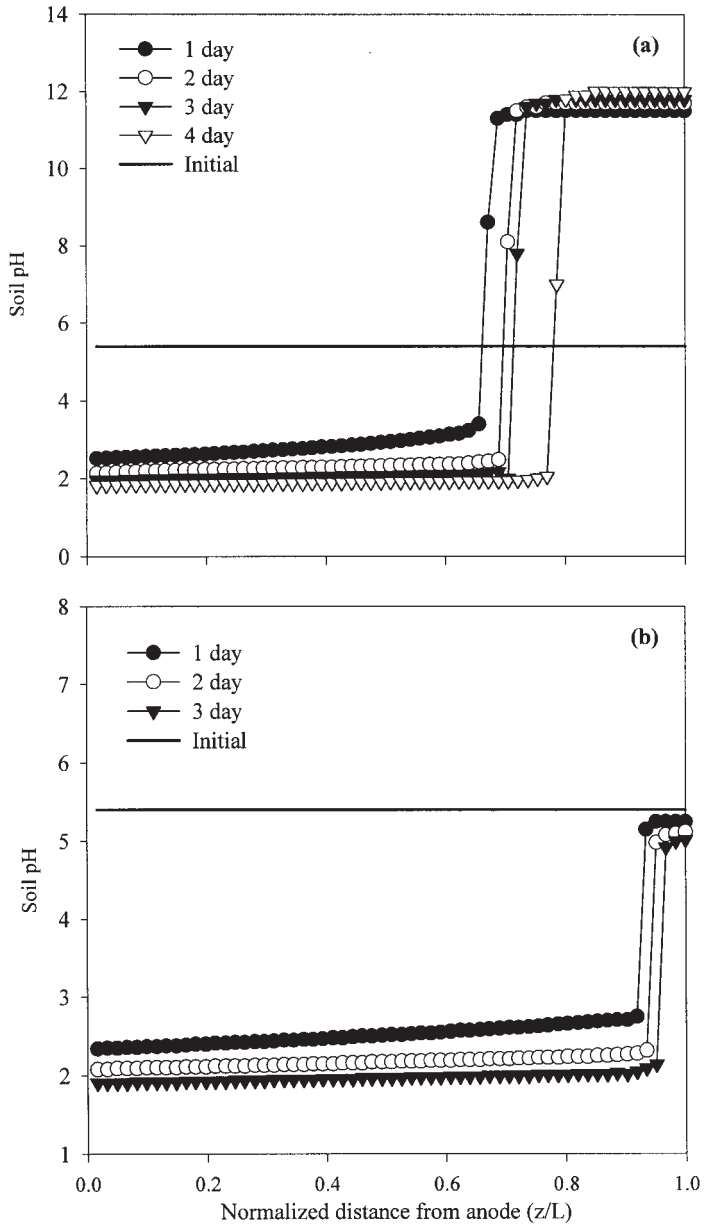

Figure 4. Model predictions of soil pH profiles in (a) the unenhanced simulation and (b) the enhanced simulation (z, distance from anode and L, length of soil cell).

Marcel Dekker, Inc.
270 Madison Avenue, New York, New York 10016

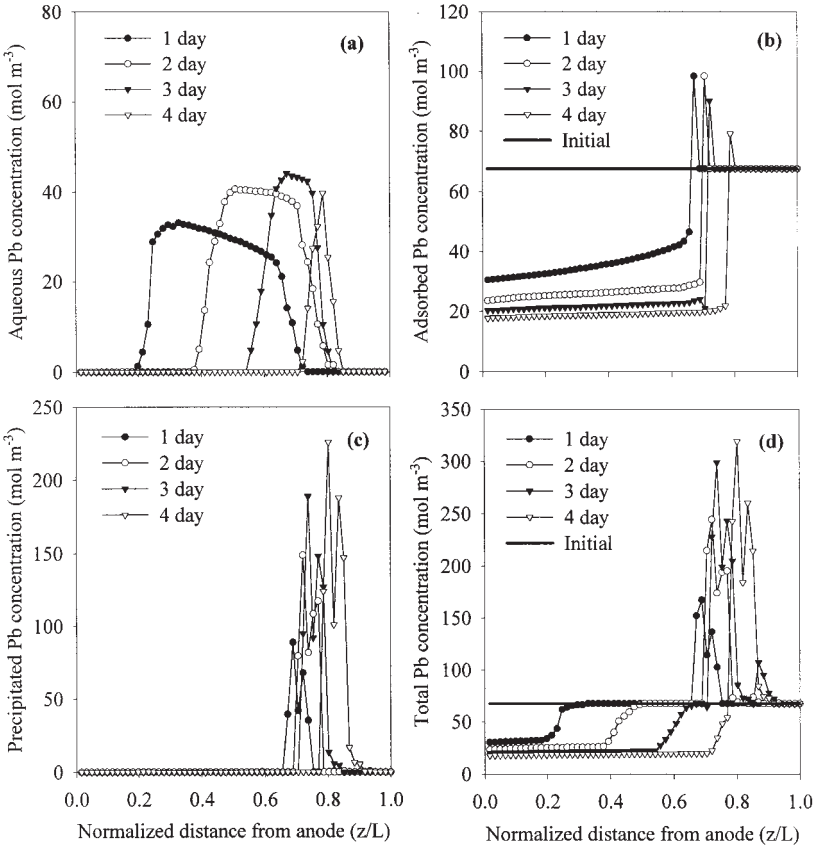

Figure 5. Model predictions of concentration profiles of different forms of Pb(II) in the unenhanced simulation: (a) aqueous form; (b) adsorbed form; (c) precipitated form; and (d) total concentration (z, distance from anode and L, length of soil cell).

adsorbed species. According to the linear and pH-dependent adsorption isotherm of Pb(II) shown in Fig. 3(b), all the adsorbed Pb(II) species can be desorbed and converted into aqueous phase species if the soil pH decreases below about 1. However, the soil pH does not decrease so much (Fig. 4), and all the adsorbed species cannot be converted into the aqueous species within most of the soil bed [Figs. 5(b) and 6(b)]. Because the soil pH decreases down to around 2 (Fig. 4), the maximum concentration of the aqueous species cannot exceed around 70% of the total concentration, i.e., $47.3\,\mathrm{mol/m^3}$, as calculated from the linear adsorption isotherm [Fig. 3(b)]. In addition, it is obvious that transport of the aqueous species is significantly delayed due to

MARCEL DEKKER, INC.
270 Madison Avenue, New York, New York 10016

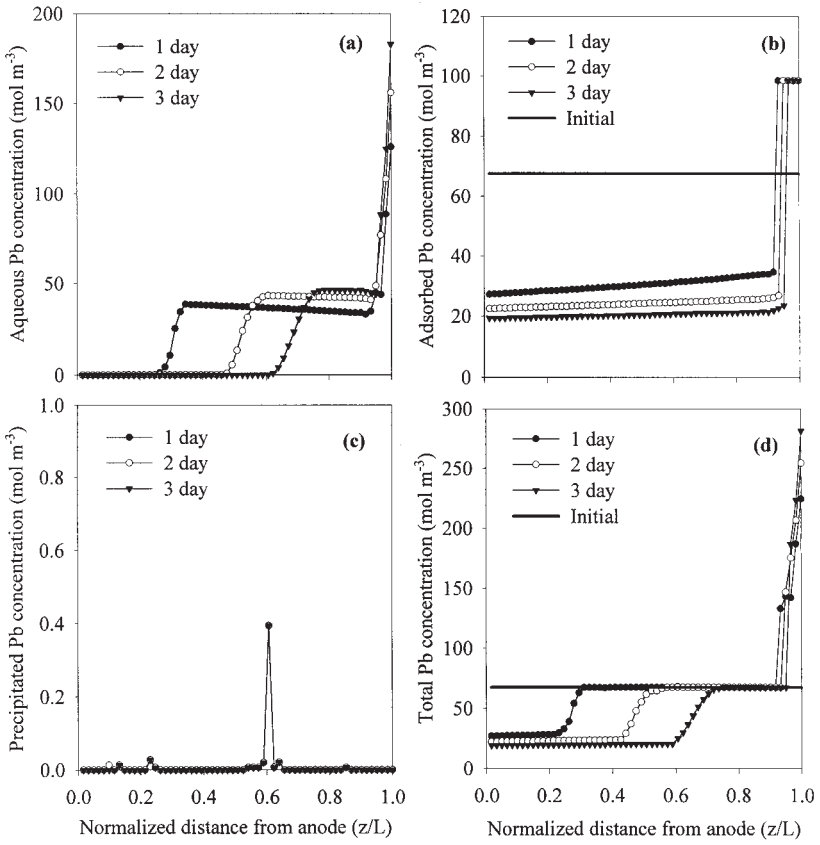

Figure 6. Model predictions of concentration profiles of different forms of Pb(II) in the enhanced simulation: (a) aqueous form; (b) adsorbed form; (c) precipitated form; and (d) total concentration (z, distance from anode, and L, length of soil cell).

the high adsorption affinity onto kaolinite surface, as shown in Fig. 5(a), even though Pb(II) has the largest ionic mobility among divalent heavy metals. On the contrary, the aqueous species more rapidly transport in the enhanced simulation than in the unenhanced simulation, because the soil pH decreases more rapidly and the adsorbed species are easily released into the pore fluid in the enhanced removal test as a result of the addition of 0.001 M acid into the analyte. The adsorbed and precipitated species are accumulated within the high pH region in the unenhanced simulation [Fig. 5(b) and (c)], whereas they are significantly decreased in the enhanced simulation [Fig. 6(b) and (c)]. A number of concentration peaks appear in the concentration profiles of the

adsorbed species of the unenhanced test [Fig. 5(b)], resulting from the pH fluctuation due to the continuous consumption of hydroxyl ions by the precipitation reaction in that region. On the other hand, multipeaked precipitations curves in Fig. 5(c) were caused by the coupled effect of local pH conditions and the constraint of the law of mass action. The local pH conditions change each time step due to the transport of hydrogen and hydroxide ions and govern the concentrations of aqueous, adsorbed, and precipitated phases of lead. In addition, the amount of precipitated lead at local points should be restricted by the law of mass action expressed in Eqs. (7a) and 7(b) and 8(a) and 8(b). To say phenomenologically, if the amounts of aqueous lead species and hydroxide ions are larger at certain local point [e.g., the former peak in Fig. 5(c)] than at other points [e.g., the latter peak in Fig. 5(c)] and those amounts satisfy the law of mass action, then two different peaks appear. It can be explained by the fact that the aqueous lead species and hydroxide ions migrate from the anodic and cathodic sides, respectively, and those two species have different ionic mobilities, while in turn the different amounts of those two species appear at each local point and finally the amount of precipitated lead is determined by the law of mass action. Accordingly, the multipeaked precipitations curves can be shown in the simulation. As shown in Fig. 5(d), the total concentration near the cathode region increases more than five times the initial concentration after the unenhanced simulation, and that concentration can be mainly attributed to the adsorbed and the precipitated forms of Pb(II). Accordingly, the final total amount of Pb(II) accumulated in that region cannot be easily removed in the unenhanced processing, even though the simulation is extended. For this reason, the unenhanced (conventional or standard) electrokinetic technology can be considered as electroaccumulation or electroconcentration processing rather than extraction or separation processing. In the case of the enhanced simulation, however, the final total amount of Pb(II) near the cathode is mainly contributed to the accumulated amount of the aqueous species migrating from the anodic side, and therefore it can be decreased with the extended running of the simulation. Consequently, the enhancement technique in electrokinetic processing is successfully used to avoid the precipitation occurring in the zone of high pH near the cathode. The effectiveness of the enhanced treatment is verified by comparison of the predictions between the unenhanced and the enhanced simulations.

Comparison of Model Predictions and Experimental Results

The predominant process controlling the contaminant transport through soils under electric fields is the electrolysis of water at both electrodes,

Marcel Dekker, Inc.
270 Madison Avenue, New York, New York 10016

which results in the formation of hydrogen ions and oxygen gas at the anode and hydroxyl ions and hydrogen gas at the cathode. An acid front moves across the soil specimen from the anode toward the cathode, while a base front migrates from cathode to anode. The acid front moves faster than the base front because the ionic mobility of hydrogen ions exceeds that of hydroxyl ions and because the direction of electroosmotic flow is toward the cathode in the high pH region above zero point of charge (zpc), i.e., in the region where soil surface has negative zeta potential. After a while, the soil under electric fields usually becomes more acidic throughout most of its volume, except close to the cathode; where the acid and base fronts meet, a sharp change in pH occurs due to the formation of water, which affects the solubilities of contaminants and their adsorption onto the soil surface. If the soil itself is highly buffered or alkaline, however, such acid front migration effect is minimized. Like this, conditioning of catholyte by the addition of acid is also effective because the hydroxyl ions generated by the water electrolysis at the cathode can be continuously buffered to prevent the hydroxide precipitation. In order to assess the effectiveness of the enhanced processing, conditioning of catholyte using nitric acid was examined in this study. The differences between the unenhanced and the enhanced processes are drastically observed in both soil pH and Pb(II) concentration profiles (Fig. 7). The comparison of the numerically simulated soil pH profiles with experimental results shows a reasonable agreement [Fig. 7(a)]. The general trend of pH distribution across the soil bed in relation to the acid and base front is shown in both numerical and experimental results, particularly in the unenhanced test. In addition, a drastic difference is visualized in between the unenhanced and enhanced tests; numerical and experimental results demonstrate that a sharp change in soil pH is nullified in the enhanced test as a result of addition of nitric acid into catholyte. The movement of the acid front is slightly faster in the numerical simulation than in the experimental measurement, possibly due to the inaccurate consideration of retardation factor for transport of hydrogen ions and the exclusion of kaolinite pH buffering capacity in simulations.

Figure 7(b) presents the final distributions of total Pb(II) concentrations numerically predicted and experimentally measured, showing that the model predictions and experimental results are reasonably in good agreement. The different profiles are clearly shown between the unenhanced and enhanced tests, particularly in the zone near the cathode, where the normalized distance from the anode is 0.6–0.78, the Pb(II) concentrations in the enhanced condition are higher than those in the unenhanced condition [Fig. 7(b)], even though the pH values are almost equivalent in that region [Fig. 7(a)]. It is caused by the different operational times between the two simulations, i.e., the operational time of the unenhanced test (4 days) was larger than that of

Marcel Dekker, Inc.
270 Madison Avenue, New York, New York 10016

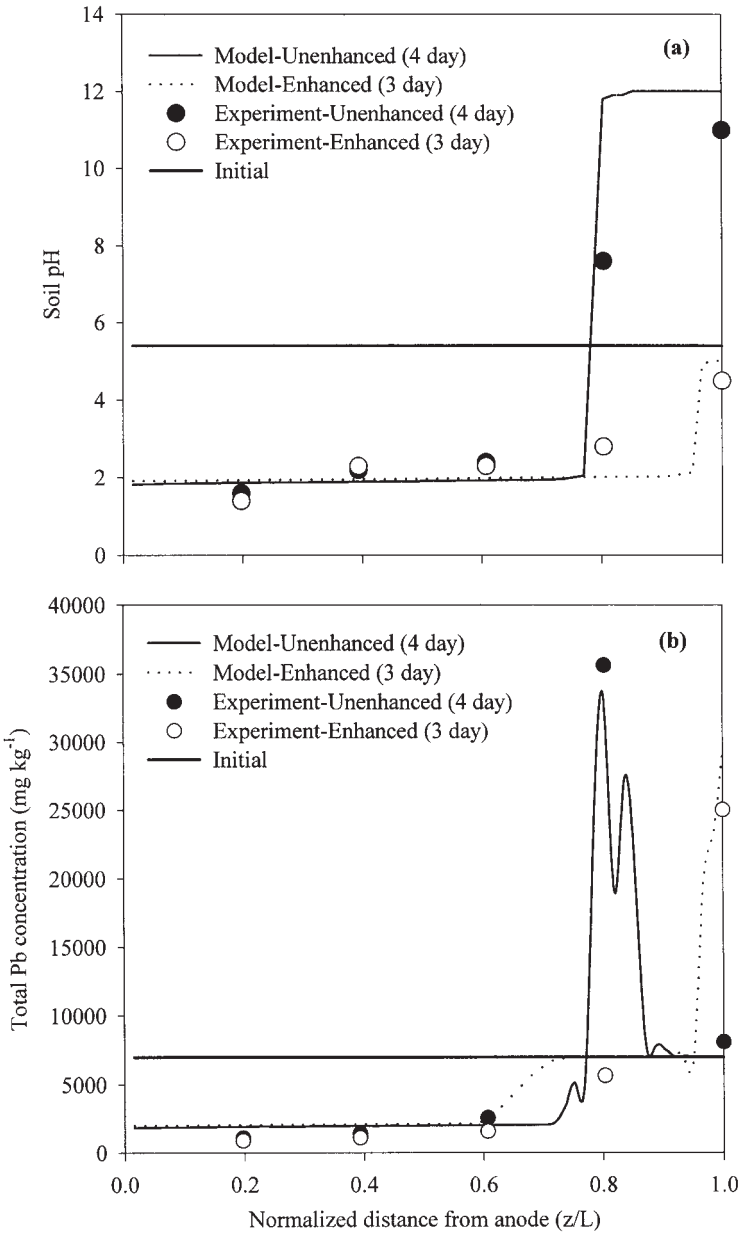

Figure 7. Comparison between model predictions and experimental results: (a) pH profiles; and (b) total Pb(II) concentrations in soil cell after treatment (z, distance from anode and L, length of soil cell).

the enhanced simulation (3 days); these different operational times caused the difference of the Pb(II) species contributing the total concentrations in that region. Comparing the major phase of Pb(II) in that region between both simulations, the amount of the aqueous species shows a significant difference [see Figs. 5(a) and 6(a)], i.e., that of the enhanced simulation is much larger than that of the unenhanced simulation, because 3 days in the enhanced simulation is not enough operational time to sweep all the aqueous. A major discrepancy between the model predictions and the experimental results is observed near the cathode. This suggests that it should be more deliberated to describe the more reasonable change in pH, adsorption, and precipitation reactions in the region near the cathode in model simulations. In addition, the hydrolytic products of lead should be considered. Over the pH ranges considered, $PbOH^{+}$, $Pb(OH)_2^0$, and $Pb(OH)_3^-$ may be important species whose mobilities are significantly different from thet of Pb^{2+}. More importantly, these hydrolytic products may increase the overall solubility of Pb(II).

CONCLUSIONS

In order to simulate Pb(II) removal from kaolinite clay using electrokinetic technique, a numerical model based on the one-dimensional diffusion–advection equation was examined in this study. The model considered multicomponent species transport under electrical and chemical gradients as well as coupled chemical reactions, such as electrolysis of water, aqueous phase reaction, adsorption, and precipitation, to describe the transport of different Pb(II) species across the soil specimen under electric fields. In particular, two different simulations (unenhanced vs. enhanced tests) were undertaken to theoretically highlight the main drawback of the unenhanced (conventional) electrokinetic processing and to assess the enhanced processing using a simple enhancement, acidic conditioning of catholyte. The unenhanced simulation clearly showed the major defect of the conventional electrokinetic processing, e.g., a sharp pH jump and precipitation of Pb(II) species in the region near the cathode as a result of migration of hydroxyl ions generated by electrolysis of water at the cathode. On the contrary, those problems were settled in the enhanced simulation. The numerical predictions for soil pH and Pb(II) concentration profiles were generally in good agreement with the experimental results, except for a slight discrepancy near the cathode. More deliberated consideration of factors controlling the changes in soil pH, adsorption, hydrolytic products of lead, and precipitation near the cathode is required in the numerical modeling.

This study clearly demonstrates that successful clean-up of Pb(II)-contaminated kaolinte clay by electrokinetic technique depends on

MARCEL DEKKER, INC.
270 Madison Avenue, New York, New York 10016

avoiding the precipitation of Pb(II) hydroxides near the cathode through the maintenance of metal ion solubility. Consequently, control of pH is of great importance in electrokinetic removal of heavy metals.

NOMENCLATURE

A	cross-sectional area of the electrodes ($0.01\ m^2$)
c_i	concentration in aqueous phase for the ith chemical species (mol/m^3)
c_{H}^{anode}	initial concentration of H^+ in the anode compartment
$c_{OH}^{cathode}$	initial concentration of OH^- in the cathode compartment
D_i	diffusion coefficient for the ith chemical species in free solution (mol/m^3)
D_i^*	effective diffusion coefficient for the ith chemical species (m^2/sec)
F	Faraday's constant ($96{,}485\ C/mol$)
I	electric current density applied in the system ($10\ A/m^2$)
J_w	electroosmotic flow rate (m/sec)
k_{eo}	electoosmotic permeability coefficient ($m^2/V\ sec$)
L	length of the soil cell
n	porosity of soil
R	universal gas constant ($8.3144\ J/K\ mol$)
R_i	production rate of the ith chemical species due to chemical reactions
R_i^{aq}	production rate of the ith chemical species due to aqueous phase reaction
R_i^{ad}	production rate of the ith chemical species due to adsorption reaction
R_i^{p}	production rate of the ith chemical species due to precipitation reaction
R_H^d	retardation factor of H^+
T	absolute temperature (K)
t	simulation time
u_i	ionic mobility for the ith chemical species at finite dilution ($m^2/V\ sec$)
u_i^*	effective ionic mobility for the ith chemical species ($m^2/Vsec$)
V_{anode}	initial volume of anolyte in the anode reservoir
$V_{cathode}$ initial	volume of catholyte in the cathode reservoir
V_{eo}	volume of water transported from anode to cathode by electroosmotic flow
z_i	charge for the ith chemical species

MARCEL DEKKER, INC.
270 Madison Avenue, New York, New York 10016

Greek Symbols

ε	permittivity of the medium (F/m)
ζ	zeta potential (V)
η	lumped parameter
μ	viscosity of fluid (N sec/m^2)
τ	tortuosity factor of the soil medium
Φ	electric potential (V)

ACKNOWLEDGMENT

This work was supported by the Postdoctoral Fellowship Programs of Korea Science & Engineering Foundation (KOSEF) and by Brain Korea 21 Program at the Department of Earth and Environmental Sciences in Korea University from the Ministry of Education. We also acknowledge the support from KOSEF through the Environmental Geosphere Research Lab (EGRL) of Korea University. The second author (JJK) was supported by the Climate Environment System Research Center sponsored by KOSEF.

REFERENCES

1. Acar, Y.B.; Alshawabkeh, A.N. Principles of electrokinetic remediation. Environ. Sci. Technol. **1993**, *46*, 2638–2647.
2. Lageman, R. Electroreclamation: applications in the Netherlands. Environ. Sci. Technol. **1993**, *27*, 2648–2650.
3. Acar, Y.B.; Gale, R.J.; Alshawabkeh, A.N. Electrokinetic remediation: basics and technology status. J. Hazard. Mater. **1995**, *40*, 117–137.
4. Alshawabkeh, A.N.; Yeung, A.T.; Bricka, M.R. Practical aspects of in-situ electrokinetic extraction. J. Environ. Eng. **1999**, *125*, 27–35.
5. Zagury, G.J.; Dartiguenave, Y.; Setier, J.C. Ex situ electroreclamation of heavy metals contaminated sludge: pilot scale study. J. Environ. Engrg **1999**, *125*, 972–978.
6. Li, R.S.; Li, L.Y. Enhancement of electrokinetic extraction from lead-spiked soils. J. Environ. Eng. **2000**, *126*, 849–857.
7. Kim, S.O.; Moon, S.H.; Kim, K.W. Enhanced electrokinetic soil remediation for removal of organic contaminants. Environ. Technol. **2000**, *21*, 417–426.

MARCEL DEKKER, INC.
270 Madison Avenue, New York, New York 10016

8. Kim, S.O.; Moon, S.H.; Kim, K.W. Removal of heavy metals from soils using enhanced electrokinetic soil processing. Water Air Soil Pollut. **2001**, *125*, 259–272.
9. Kim, S.O.; Kim, K.W.; Stüben, D. Evaluation of electrokinetic removal of heavy metals from tailing soils. J. Environ. Eng. **2002**, *128*, 705–715.
10. Page, M.M.; Page, C.L. Electroremediation of contaminated soils. J. Environ. Eng. **2002**, *128*, 208–219.
11. Virkutyte, J.; Sillanpää, M.; Latostenmaa, P. Electrokinetic soil remediation-critical overview. Sci. Total Environ. **2002**, *289*, 92–121.
12. Baraud, F.; Tellier, S.; Astruc, M. Temperature effect on ionic transport during soil electrokinetic treatment at constant pH. J. Hazard. Mater. **1999**, *64*, 263–281.
13. Kim, S.O. Electrokinetic Remediation of Heavy Metal Contaminated Soils and Sludges. Kwangju Institute of Science and Technology: Kwangju, Republic of Korea, 2001, 9–12; Ph.D. Dissertation.
14. Mitchell, J.K. *Fundamentals of Soil Behavior*; John Wiley & Sons, Inc.: New York, 1993; 336–337.
15. Davies, B.E. Lead. In *Heavy Metals in Soil*; Alloway, B.J., Ed.; Blackie Academic & Professional: London, UK, 1995; 206–223.
16. Venema, P.; Hiemstra, T.; Weidler, P.G.; Van Riemsdijk, W.H. Intrinsic proton affinity of reactive surface groups of metal (hydro)oxides: application to iron (hydro)oxides. J. Colloid Interface Sci. **1997**, *198*, 252–295.
17. Li, L.Y.; Wu, G. Numerical simulation of transport of four metals in kaolinte clay. J. Environ. Eng. **1999**, *125*, 314–324.
18. Christophi, C.A.; Axe, L. Competition of Cd, Cu, and Pb adsorption on goethite. J. Environ. Eng. **2000**, *126*, 66–74.
19. Probstein, R.F. *Physicochemical Hydrodynamics—An Introduction*; John Wiley & Sons, Inc.: New York, 1994; 190–208.
20. Alshawabkeh, A.N.; Acar, Y.B. Electrokinetic remediation. II: Theoretical model. J. Geotech. Eng. **1996**, *122*, 186–196.
21. Eykholt, G.R.; Daniel, D.E. Impact of system chemistry on electroosmosis in contaminated soils. J. Geotech. Eng. **1994**, *120*, 797–815.
22. Shapiro, A.P.; Probstein, R. Removal of contaminants from saturated clay by electroosmosis. Environ. Sci. Technol. **1993**, *27*, 283–291.
23. Alshawabkeh, A.N. Theoretical and Experimental Modeling of Removing Contaminants from Soils by an Electric Field. The Louisiana State University: Baton Rouge, LA, 1994; Ph.D. Dissertation.
24. Daniel, D.E. *Geotechnical Practice for Waste Disposal*; Chapman & Hall: London, UK, 1993; 33–65.

MARCEL DEKKER, INC.
270 Madison Avenue, New York, New York 10016

25. Daniel, D.E.; Shackelford, C.D. Disposal barriers that release contaminants only by molecular diffusion. Nucl. Chem. Waste Man. **1988**, *8*, 299–305.
26. Shackelford, C.D. Diffusion of contaminants through waste containment barriers. Transportation Research Record 1219, Transportatin Resrach Board, National Research Council, Washington, DC, 1989; 169–182.
27. Shackelford, C.D.; Daniel, D.E. Diffusion in saturated soil: I. Background. J. Geotech. Eng. **1991**, *117*, 467–484.
28. Holmes, P.J. *The Electrochemistry of Semiconductors*; Academic Press: London, UK, 1962; 396 pp.
29. Shapiro, A.P. Electroosmotic Purging of Contaminants from Saturated Soils. Massachusetts Institute of Technology: Cambridge, MA, 1990; Ph.D. Dissertation.
30. Shapiro, A.P.; Probsten, R. Removal of contaminants from saturated clay by electroosmosis. Environ. Sci. Technol. **1993**, *27*, 283–291.
31. Hsu, C.N. Electrokinetic Remediation of Heavy Metal Contaminated Soils. Texas A&M Univ., College Station: TX, 1997; Ph.D. Dissertation.
32. Acar, Y.B.; Alshawabkeh, A.N. Electrokinetic remediation. I: pilot-scale tests with lead-spiked kaolinite. J. Geotech. Eng. **1996**, *122*, 173–185.
33. Jacobs, R.A.; Probstein, R.F. Two-dimensional modeling of electroremediation. AIChE J. **1996**, *42*, 1685–1696.
34. Eykholt, G.R. Driving and Complicating Features of Electrokinetic Treatment of Soils. University of Texas: Austin, TX, 1992; Ph.D. Dissertation.
35. Lorenz, P.B. Surface conductance and electrokinetic properties of kaolinite beds. Clay. Clay Miner. **1969**, *17*, 223–231.

Received April 2003
Accepted December 2003